JACS
JOURNAL OF THE AMERICAN CHEMICAL SOCIETY

Communication

pubs.acs.org/JACS

Controlled Self-Assembly of Organic Composite Microdisks for Efficient Output Coupling of Whispering-Gallery-Mode Lasers

Cong Wei,[†] Si-Yun Liu,[†] Chang-Ling Zou,[‡] Yingying Liu,[†] Jiannian Yao,[†] and Yong Sheng Zhao*,[†]

[†]Beijing National Laboratory for Molecular Sciences, Institute of Chemistry, Chinese Academy of Sciences, Beijing 100190, China
[‡]Key Laboratory of Quantum Information, University of Science and Technology of China, Hefei 230026, Anhui, China

Supporting Information

ABSTRACT: Flexible microdisk whispering-gallery-mode (WGM) resonators with high quality factors were achieved through the controlled assembly of organic materials with an emulsion-solvent-evaporation method. The high material compatibility of the assembled microdisks enabled us to realize low-threshold WGM lasers by doping with organic dyes as gain media. Furthermore, the emulsion-assisted self-assembly provided a strategy for the one-step fabrication of microwire-waveguide-connected microdisk heterostructures, which can be utilized for the efficient output of the isotropic WGM lasers from the coupled waveguides. We hope that these results will pave an avenue for the construction of new types of flexible WGM-based components for photonic integration.

With high quality (Q) factors and small mode volumes, whispering-gallery-mode (WGM) microcavities can tightly confine photons for a long time by means of continuous total internal reflection along a smooth, curved surface, making them ideal candidates for novel coherent light sources[1] that hold promising applications in high-throughput sensing[2] and on-chip optical communication.[3] With the development of top-down processing techniques, various shaped solid cavities have been achieved, including disks,[4,5] rings,[6,7] and toroidals,[8] supporting effective optical feedback for the lasing emission.[4,6,9] However, these resonators require sophisticated planar epitaxial technology to incorporate the optical gain medium.[4,5] The strict requirement of lattice matching between the epitaxial layers limits the choice of gain materials, posing a formidable challenge to design and tailor the lasing wavelengths of these cavities.

In comparison, with outstanding doping flexibility, organic matrixes can be expediently incorporated with various laser dyes as optical gain media.[10] The emission wavelengths of these dyes can be easily tuned from UV to near-IR through molecular design.[11,12] Furthermore, the chemical versatility and flexible nature of organic materials allow for numerous kinds of micro/nanoassemblies,[13,14] even highly bent waveguides,[15,16] microrings,[17,18] isotropic spheres,[19,20] platelets,[21] and hemispheres,[22,23] where the light would be well confined via the formation of WGM resonance. To this end, organic materials would be ideal for the fabrication of flexible WGM microresonators to realize lasing emission over the whole visible spectrum. However, constructing organic WGM resonators in a controlled way, which is critically important for tailoring their resonant modes[24] and efficiently collecting their emission,[25] is still a challenge.

Here we propose a strategy to produce highly flexible microdisk WGM resonators based on the controlled emulsion assembly of organic materials. The diameter of the microdisk can be finely tuned by altering the micelle size of the emulsion during the assembly process. With an ultrasmooth surface and perfect circle boundary, the acquired microdisk possesses a Q factor of over several thousand and can provide sufficient feedback for the laser oscillations. Because organic materials with strong intermolecular interactions exhibit excellent compatibility, we chose appropriate guest organic laser dyes that have strong interactions with the host material of the microdisk to dope into these WGM resonators and realized low-threshold WGM lasers under optical pumping. Further, the lasing emission was efficiently output from a tangentially coupled wire waveguide that was obtained by one-step assembly via a controllable phase separation between the doped dye and the matrix material. The results offer a comprehensive understanding of the assembly mechanism of organic composite materials and open a new way to construct flexible WGM-based photonic components[26] that can be integrated with other functional devices.

The organic WGM resonators were obtained by controllably evaporating the solvent of the emulsion solution containing the isotropic spherical micelles (see the Supporting Information (SI) for details). Polystyrene (PS), which is transparent in the visible range, was chosen as the matrix material to create the high-quality microdisk resonators because of its outstanding flexibility. Our concept for the generation of PS microdisks is illustrated in Figure 1A. First, PS molecules were dissolved in *N*,*N*-dimethylformamide (DMF), and then slow precipitation of PS was induced by adding a small amount of water.[27] Driven by the interfacial tension, the polymer molecules with low crystallinity prefer to aggregate into spherical micelles.[19] Thus, a PS microemulsion was achieved after ultrasonic treatment, as confirmed by enhanced light scattering intensity of the polymer solution (Figure S1 in the SI). To obtain the disk-shaped resonators, we subsequently used a tiny gap consisting of two glass substrates as a template during drying of the PS micelles. The capillary force in the tiny gap squashed these spherical micelles into disk-shaped structures.

The corresponding optical microscopy (OM) images in Figure 1A show that large-scale microstructures with circular boundaries were obtained after complete evaporation of the solvent. The disk shape was confirmed by top- and side-view scanning electron microscopy (SEM) images (Figure S2). According to

Received: November 3, 2014
Published: December 24, 2014

DOI: 10.1021/ja5112817
J. Am. Chem. Soc. 2015, 137, 62−65

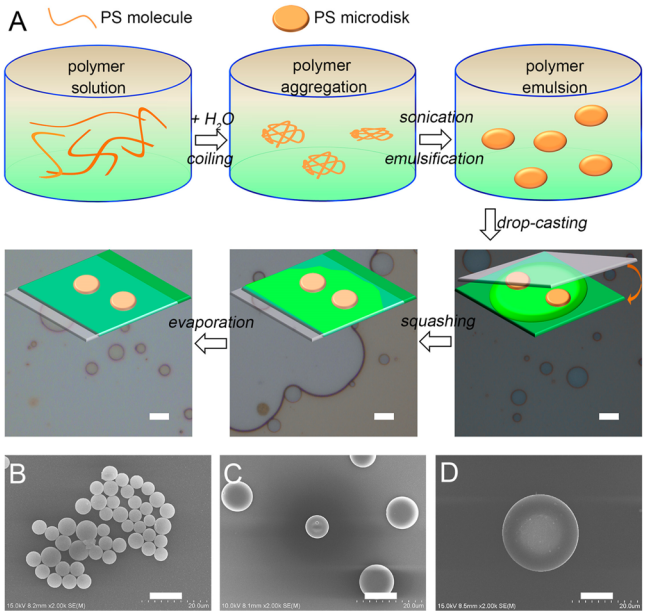

Figure 1. (A) Schematic diagram of the microdisk fabrication process. Corresponding OM images are also shown. (B–D) SEM images of the PS microdisks prepared by adding water (10, 20, and 30 μL, respectively) to the PS solution (1 mL). All scale bars are 10 μm.

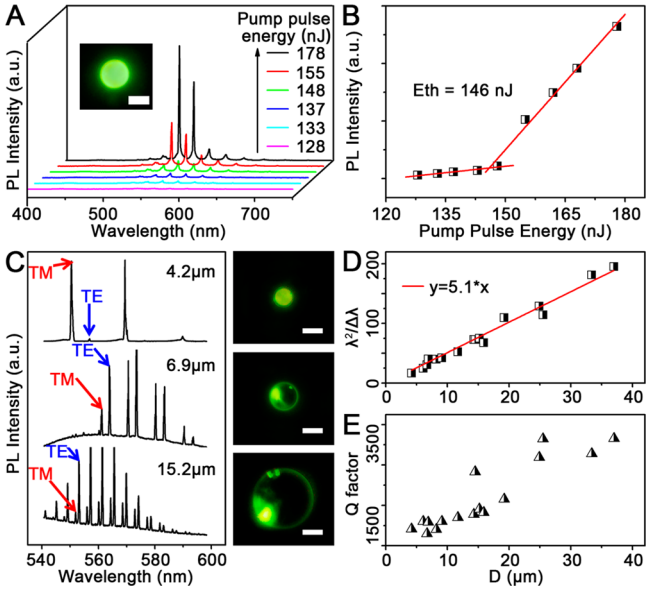

Figure 2. WGM lasing characteristics of the dye-doped PS microdisks. (A) PL spectra recorded at the edge of a microdisk as a function of pump energy. Inset: PL image of the microdisk under laser excitation. The scale bar is 5 μm. (B) Plots of PL peak intensity vs excitation pulse energy. (C) PL spectra of microdisks with different diameters and corresponding PL images. TE and TM are labeled according to the polarization-sensitive PL spectra illustrated in Figure S6. Scale bars are 10 μm. (D) Relationship between $\lambda^2/\Delta\lambda$ and the diameter of the microdisk (D). The red line is a fit to the function $\lambda^2/\Delta\lambda = n\pi D$. (E) Plot of experimental Q factor vs microdisk diameter.

our proposed assembly process, the diameter of the microdisks is in direct proportion to the size of the micelles in the emulsion solution. The size should strongly depend on the interfacial tension between PS and the solvent phase, which increases with the volume of water added, generating larger polymer micelles with smaller specific surface areas to reduce the interfacial energy of the system. Thus, we could finely tune the microdisk diameter from 4 to 20 μm by changing the amount of water added from 10 to 30 μL mL^{-1} (Figure 1B–D).

The microdisks have a perfect circlular boundary and ultrasmooth surface, which is favorable for WGM resonance. Moreover, the phenyl groups of the PS matrix may have a strong $\pi-\pi$ interactions with π-conjugated molecules, resulting in excellent compatibility with conjugated chromophores. This enabled us to realize WGM lasers by doping luminescent dyes into the microdisks. 1,4-Bis(α-cyano-4-diphenylaminostyryl)-2,5-diphenylbenzene (CNDPASDB, Figure S3), an efficient laser dye[28] with a delocalized π-conjugated system, was added to the polymer solution at a concentration of ~1 wt % relative to PS, providing the optical gain for the operation of the WGM laser. The composite microdisks emitted uniform yellow fluorescence of CNDPASDB under UV excitation (Figure S4), confirming uniform doping of the dye in the PS matrix.

When the dye-doped microdisk was excited locally with a focused pulsed laser beam (400 nm, ~200 fs) in a homemade microphotoluminescence system (Figure S5), a brighter ring shape pattern located at the outer boundary of the microdisk was observed (Figure 2A inset), indicating total internal reflection of the emitted light along the edge of the microdisk. A series of sharp peaks from the WGM modulation was found in the photoluminescence (PL) spectra collected from the edge of the microdisk, as shown in Figure 2A. With increasing pump pulse energy, the PL intensities of two peaks in the gain region were dramatically amplified, indicating lasing action of the polymer microdisks. The corresponding power dependence of the PL intensity (Figure 2B) showed a nonlinear behavior at the threshold of ~146 nJ pulse^{-1}. This resulted from the stimulated emission of the doped organic dye, which further confirmed the lasing action of these microdisks.

The lasing characteristics of these flexible WGM resonators, including the mode spacing and Q factor, were well-tuned by altering the size of the microdisks. Figure 2C presents fluorescence images and spectra of three distinct microdisks with different diameters under excitation at a pump energy of 175 nJ pulse^{-1} (above their laser thresholds). Bright emission was observed along their ring-shaped boundaries, which is the typical characteristic of the formation of WGM resonance. All of the spectra show two separated lasing envelopes as a result of the breakdown of the degeneracy of the transverse electric (TE) and transverse magnetic (TM) modes in the microdisks.[24] This was further verified by the spatially resolved polarization-sensitive PL spectra (Figure S6). Both the TE and TM mode spacings ($\Delta\lambda$) gradually increase with decreasing microdisk diameter (D), providing an opportunity to achieve single-mode lasers. According to the WGM theory, the mode spacing $\Delta\lambda$ and the diameter D should satisfy the equation $\lambda^2/\Delta\lambda = n\pi D$, where λ is the wavelength of the guided light and n is the group refractive index. On the basis of the experimentally measured relationship between $\lambda^2/\Delta\lambda$ and D (Figure 2D), $n = 1.62$ was obtained, which is consistent with the intrinsic refractive index of the PS polymer (1.59). This indicates that the optical WGM modes are tightly confined in the polymer matrix with negligible optical leakage to the substrate, which is beneficial for resonators with high Q factors. The measured Q factors of the microdisks were on the order of 10^3 to 10^4, which is pretty high for organic resonators (Figure 2E).[22,29] The Q factor increased with increasing D because the bending radiation loss of circular resonators declines exponentially with their size.[30]

DOI: 10.1021/ja5112817
J. Am. Chem. Soc. 2015, 137, 62–65

With high Q factors and tight optical confinement, these doped flexible microdisks can serve as ideal resonators for achieving low-threshold miniaturized lasers. However, their perfect rotational symmetry results in isotropic emission (Figure S7), which is undesired for the integration with other functional components. To design a proper structure for breaking the symmetry and efficiently collecting the WGM signals, we employed a two-dimensional finite-difference time-domain (FDTD) method to simulate the spatial field distributions of the microdisks. As illustrated in Figure 3A, the electric field in a discrete microdisk is symmetrically distributed. Comparatively, when a disk is connected with a tangent waveguide, there is strong coupling between them that can be used to efficiently export the resonating light.

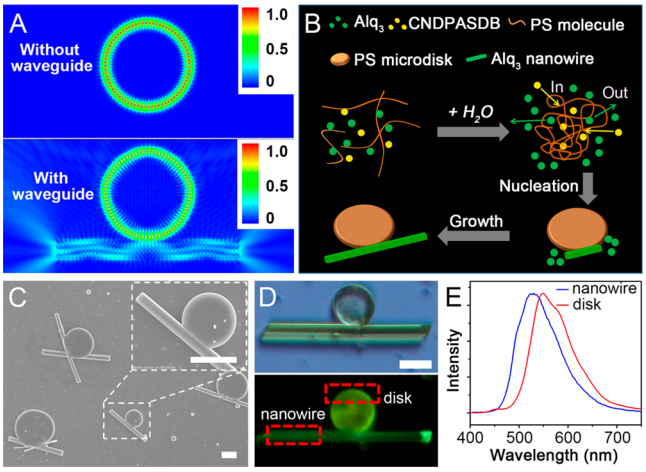

Figure 3. (A) Spatial distributions of the WGM in the microdisk resonator with and without the connected waveguide. (B) Schematic illustration of the proposed assembly strategy to create the tangent waveguide on the microdisk WGM resonator. (C) SEM images of the acquired microwire-connected microdisks. Inset: magnified SEM image showing the junction between the disk and the wire. Scale bars are 10 μm. (D) Bright-field image (top) and corresponding PL image (bottom) of the wire-connected disk under UV excitation. The scale bar is 5 μm. (E) Spatially resolved PL spectra collected from the wire and disk shown in (D).

It was reported that waveguide-coupled WGM resonators can be achieved by using precisely aligned tapered fibers[31] or etching techniques,[32] which require sophisticated multistep procedures. The emulsion assembly method proposed in this work provides a strategy for the one-step construction of waveguide-coupled microdisks for the efficient output coupling of WGM lasers. Although the PS matrix has good compatibility with π-conjugated CNDPASDB, upon the introduction of a dye compound with a nonplanar molecular structure, the weaker interaction will lead to phase separation during the self-assembly to give a hybrid structure. Here we applied aluminum tris(8-hydroxyquinoline) (Alq_3) with a twisted molecular structure (Figure S3). The photographs shown in Figure S8 prove that in comparison with CNDPASDB, the nonplanar structure of Alq_3 leads to a weaker interaction with PS. We initiated the cooperative assembly of PS, CNDPASDB, and Alq_3 by dropwise addition of a small amount of water into their mixed solution (Figure 3B). During the nucleation of PS, the CNDPASDB gradually diffused into the polymer matrix, while the Alq_3 preferred to stay in the solvent phase. Upon evaporation of the solvent, the CNDPASDB-doped PS microdisks formed as mentioned above, and the Alq_3 turned to nucleate at the edge of the squashed PS microdisks because the small radius of curvature and high surface energy allow them to serve as preferential condensation nuclei.[33,34] The Alq_3 then aggregated to form 1D nanostructures via epitaxial growth driven by its own intermolecular interactions. The Alq_3-wire-coupled microdisks were obtained after aging of the assembly system for 10 h.

Figure 3C shows SEM images of some typical assembled hybrid structures. It can be seen that most of the doped microdisks were tangentially connected with a wire. Structures with disk-to-wire ratios of 1:2 or more could also be obtained with higher concentrations of Alq_3 in the mixed solution. Temporal observation of the assembly process (Figure S9) showed that with solvent evaporation, doped disks formed first and then provided spots for the nucleation and growth of the one-dimensional structure. Almost all of the wires were tangentially connected to the microdisks, possibly because the Alq_3 molecules preferred to aggregate along the interface between the PS micelle and the solvent phase to reduce the interface energy. Figure 3D displays bright-field and PL images of a typical hybrid structure. Under UV excitation, the disk and microwire showed different emission colors. The spatially resolved PL spectra (Figure 3E) demonstrate that the spectrum recorded from the microwire presents a single peak at 530 nm, which is identical to that of Alq_3 (Figure S10). In contrast, the spectrum of the disk shows a maximum emission at ~550 nm and a shoulder at ~580 nm, in good accordance with the emission features of CNDPASDB.

The tangentially connected heterostructure facilitates light coupling both from the waveguide to the WGM resonator and the other way. As shown in Figure S11, when the Alq_3 wire was excited locally at one end with a focused UV laser (351 nm), the light flow was steered from the excitation spot toward the other tip. Most importantly, the emission could be trapped in the microdisk at wavelengths consistent with the resonance cavity. Thus, a series of sharp dips from the WGM modulation of the microdisk was found in the spectrum outcoupled at the end of the microwire waveguide, but such a series was absent without the disk (Figure S12). The spacing between the neighboring dips was found to be in fine accordance with the mode spacing of the connected disk, further confirming the strong coupling between the wire and the disk.

On the basis of the simulation illustrated in Figure 3A, the strong coupling would break down the rotational symmetry of the cavity and help to efficiently output the WGM laser from the wire. As displayed in Figure 4A, when a 400 nm femtosecond-pulsed laser beam was focused at the disk edge, bright PL spots were observed at the tips of the wire. The spectra shown in Figure 4B indicate that the WGM laser with CNDPASDB as the gain medium was effectively outcoupled from the wire waveguide without obvious signal distortion. As an important signal carrier in optical communication, the polarization state is a key character of the lasing emission. In the microdisk resonator, the TE and TM modes are polarized parallel and perpendicular to the disk plane, respectively,[35] as shown by the polarization detection results in Figure 4C. Both the TE and TM lasing modes output from the wire tip maintained their polarizations very well (Figure 4D). These results reveal that the self-assembled structures demonstrated in this work can be applied to realize efficient output coupling of WGM lasers without changing the intrinsic properties (wavelength, polarization, etc.), which is of great significance for the integration of the WGM laser with other functional photonic components.

DOI: 10.1021/ja5112817
J. Am. Chem. Soc. 2015, 137, 62−65

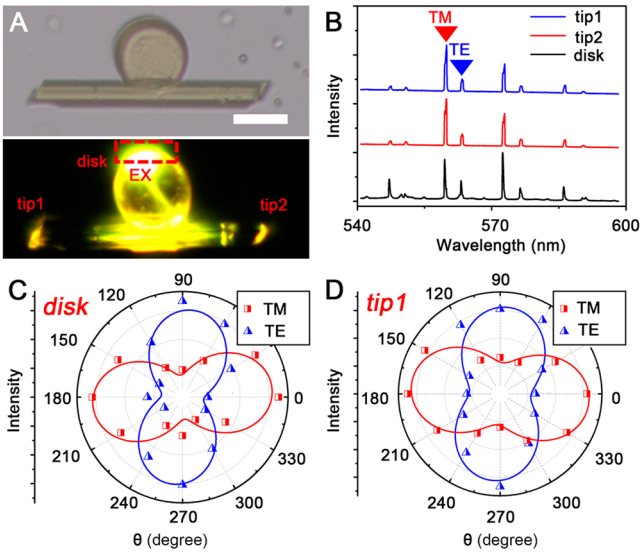

Figure 4. (A) Bright-field and PL images of a wire-connected microdisk locally excited at the disk edge with a pulsed laser. EX denotes the excitation position. The scale bar is 5 μm. (B) Spatially resolved PL spectra collected from the disk and the wire tips, as marked in (A). (C, D) Spatial polarization profiles of the emission intensities of the TM and TE lasing modes collected from (C) the disk and (D) the wire tip as marked in (A). θ refers to the angle between the polarizer transmission direction and the axis of the wire.

In summary, we have reported a facile emulsion-solvent-evaporation method to construct highly flexible organic microdisk resonators in a controlled way. The microdisks can confine the light well via the formation of WGM resonance. By incorporation of a laser dye having excellent compatibility with the microdisk matrix, low-threshold WGM lasing was obtained under optical pumping. Furthermore, on the basis of our proposed assembly strategy, waveguide-coupled microdisks were prepared by one-step self-assembly, and the waveguide efficiently coupled the output of the WGM laser without loss of the intrinsic properties of the signals. We anticipate that the composite microdisks could be ideal for achieving various functional nanophotonic devices and lead to useful platforms for fundamental research in nanophotonics and quantum optics.

■ ASSOCIATED CONTENT

Ⓢ Supporting Information

Experimental details and additional data. This material is available free of charge via the Internet at http://pubs.acs.org.

■ AUTHOR INFORMATION

Corresponding Author

yszhao@iccas.ac.cn

Notes

The authors declare no competing financial interest.

■ ACKNOWLEDGMENTS

This work was supported by the National Natural Science Foundation of China (21125315, 21221002), the Ministry of Science and Technology of China (2012YQ120060), and the Strategic Priority Research Program of the Chinese Academy of Sciences (XDB12020300).

■ REFERENCES

(1) Vahala, K. J. *Nature* **2003**, *424*, 839.
(2) He, L.; Özdemir, S. K.; Zhu, J.; Kim, W.; Yang, L. *Nat. Nanotechnol.* **2011**, *6*, 428.
(3) Xia, F.; Sekaric, L.; Vlasov, Y. *Nat. Photonics* **2007**, *1*, 65.
(4) Baek, H.; Lee, C.-H.; Chung, K.; Yi, G.-C. *Nano Lett.* **2013**, *13*, 2782.
(5) Chen, R.; Gupta, S.; Huang, Y.-C.; Huo, Y.; Rudy, C. W.; Sanchez, E.; Kim, Y.; Kamins, T. I.; Saraswat, K. C.; Harris, J. S. *Nano Lett.* **2014**, *14*, 37.
(6) Pauzauskie, P. J.; Sirbuly, D. J.; Yang, P. *Phys. Rev. Lett.* **2006**, *96*, No. 143903.
(7) Clark, A. W.; Glidle, A.; Cumming, D. R. S.; Cooper, J. M. *J. Am. Chem. Soc.* **2009**, *131*, 17615.
(8) Armani, D. K.; Kippenberg, T. J.; Spillane, S. M.; Vahala, K. J. *Nature* **2003**, *421*, 925.
(9) Mahler, L.; Tredicucci, A.; Beltram, F.; Walther, C.; Faist, J.; Witzigmann, B.; Beere, H. E.; Ritchie, D. A. *Nat. Photonics* **2009**, *3*, 46.
(10) Cerdán, L.; Enciso, E.; Martin, V.; Bañuelos, J.; López-Arbeloa, I.; Costela, A.; García-Moreno, I. *Nat. Photonics* **2012**, *6*, 621.
(11) Zhao, Y. S.; Peng, A.; Fu, H.; Ma, Y.; Yao, J. *Adv. Mater.* **2008**, *20*, 1661.
(12) Yu, J.; Cui, Y.; Xu, H.; Yang, Y.; Wang, Z.; Chen, B.; Qian, G. *Nat. Commun.* **2013**, *4*, No. 2719.
(13) Chandrasekar, R. *Phys. Chem. Chem. Phys.* **2014**, *16*, 7173.
(14) Yan, Y.; Zhao, Y. S. *Chem. Soc. Rev.* **2014**, *43*, 4325.
(15) Chandrasekhar, N.; Mohiddon, M. A.; Chandrasekar, R. *Adv. Opt. Mater.* **2013**, *1*, 305.
(16) Basak, S.; Chandrasekar, R. *J. Mater. Chem. C* **2014**, *2*, 1404.
(17) Takazawa, K.; Inoue, J.-i.; Mitsuishi, K.; Takamasu, T. *Adv. Mater.* **2011**, *23*, 3659.
(18) Chandrasekhar, N.; Chandrasekar, R. *Angew. Chem., Int. Ed.* **2012**, *51*, 3556.
(19) Adachi, T.; Tong, L.; Kuwabara, J.; Kanbara, T.; Saeki, A.; Seki, S.; Yamamoto, Y. *J. Am. Chem. Soc.* **2013**, *135*, 870.
(20) Tabata, K.; Braam, D.; Kushida, S.; Tong, L.; Kuwabara, J.; Kanbara, T.; Beckel, A.; Lorke, A.; Yamamoto, Y. *Sci. Rep.* **2014**, *4*, 5902.
(21) Zhang, Q.; Ha, S. T.; Liu, X.; Sum, T. C.; Xiong, Q. *Nano Lett.* **2014**, *14*, 5995.
(22) Haase, J.; Shinohara, S.; Mundra, P.; Risse, G.; Lyssenko, V. G.; Fröb, H.; Hentschel, M.; Eychmüller, A.; Leo, K. *Appl. Phys. Lett.* **2010**, *97*, No. 211101.
(23) Ta, V. D.; Chen, R.; Sun, H. D. *Adv. Mater.* **2012**, *24*, OP60.
(24) Ta, V. D.; Chen, R.; Sun, H. D. *Sci. Rep.* **2013**, *3*, 1362.
(25) Jiang, X.-F.; Xiao, Y.-F.; Zou, C.-L.; He, L. N.; Dong, C.-H.; Li, B.-B.; Li, Y.; Sun, F.-W.; Yang, L.; Gong, Q. H. *Adv. Mater.* **2012**, *24*, OP260.
(26) Takazawa, K.; Inoue, J.-i.; Mitsuishi, K.; Kuroda, T. *Adv. Funct. Mater.* **2013**, *23*, 839.
(27) Deng, R.; Liu, S.; Li, J.; Liao, Y.; Tao, J.; Zhu, J. *Adv. Mater.* **2012**, *24*, 1889.
(28) Li, Y.; Shen, F.; Wang, H.; He, F.; Xie, Z.; Zhang, H.; Wang, Z.; Liu, L.; Li, F.; Hanif, M.; Ye, L.; Ma, Y. *Chem. Mater.* **2008**, *20*, 7312.
(29) Zhang, C.; Zou, C.-L.; Yan, Y.; Hao, R.; Sun, F.-W.; Han, Z.-F.; Zhao, Y. S.; Yao, J. *J. Am. Chem. Soc.* **2011**, *133*, 7276.
(30) Zhang, C.; Zou, C.-L.; Yan, Y.; Wei, C.; Cui, J.-M.; Sun, F.-W.; Yao, J.; Zhao, Y. S. *Adv. Opt. Mater.* **2013**, *1*, 357.
(31) Yang, L.; Armani, D. K.; Vahala, K. J. *Appl. Phys. Lett.* **2003**, *83*, 825.
(32) Hausmann, B. J. M.; Shields, B.; Quan, Q.; Maletinsky, P.; McCutcheon, M.; Choy, J. T.; Babinec, T. M.; Kubanek, A.; Yacoby, A.; Lukin, M. D.; Lončar, M. *Nano Lett.* **2012**, *12*, 1578.
(33) Zheng, J. Y.; Yan, Y.; Wang, X.; Zhao, Y. S.; Huang, J.; Yao, J. *J. Am. Chem. Soc.* **2012**, *134*, 2880.
(34) Chikkaraddy, R.; Dasgupta, A.; Dutta Gupta, S.; Pavan Kumar, G. V. *Appl. Phys. Lett.* **2013**, *103*, No. 031112.
(35) Cao, H.; Xu, J. Y.; Xiang, W. H.; Ma, Y.; Chang, S.-H.; Ho, S. T.; Solomon, G. S. *Appl. Phys. Lett.* **2000**, *76*, 3519.

DOI: 10.1021/ja5112817
J. Am. Chem. Soc. 2015, 137, 62−65